

Low-loss, smile-insensitive external frequency-stabilization of high power diode lasers enabled by vertical designs with extremely low divergence angle and high efficiency

P. Crump^{*†}, S. Knigge[†], A. Maaßdorf[†], F. Bugge[†], S. Hengesbach[‡], U. Witte^β, H.D. Hoffmann^β, B. Köhler[¥], R. Hubrich[¥], H. Kissel[¥], J. Biesenbach[¥], G. Erbert[†] and G. Tränkle[†]

[†] Ferdinand-Braun-Institut, Leibniz-Institut für Höchstfrequenztechnik, Gustav-Kirchoff-Str. 4, 12489 Berlin, Germany

[‡] Chair for Laser Technology LLT, RWTH Aachen University, Steinbachstr. 15, 52074 Aachen, Germany

^β Fraunhofer-Institut für Lasertechnik, Steinbachstr. 15, 52074 Aachen, Germany.

[¥] DILAS Diodenlaser GmbH, Galileo-Galilei-Straße 10, 55129 Mainz, Germany.

ABSTRACT

Broad area lasers with narrow spectra are required for many pumping applications and for wavelength beam combination. Although monolithically stabilized lasers show high performance, some applications can only be addressed with external frequency stabilization, for example when very narrow spectra are required. When conventional diode lasers with vertical far field angle, $\Theta_v^{95\%} \sim 45^\circ$ (95% power) are stabilized using volume holographic gratings (VHG), optical losses are introduced, limiting both efficiency and reliable output power, with the presence of any bar smile compounding the challenge. Diode lasers with designs optimized for **extremely low** vertical **d**ivergence (ELOD lasers) directly address these challenges. The vertical far field angle in conventional laser designs is limited by the waveguiding of the active region itself. In ELOD designs, quantum barriers are used that have low refractive index, enabling the influence of the active region to be suppressed, leading to narrow far field operation from thin vertical structures, for minimal electrical resistance and maximum power conversion efficiency. We review the design process, and show that 975 nm diode lasers with 90 μm stripes that use ELOD designs operate with $\Theta_v^{95\%} = 26^\circ$ and reach 58% power conversion efficiency at a CW output power of 10 W. We demonstrate directly that VHG stabilized ELOD lasers have significantly lower loss and larger operation windows than conventional lasers in the collimated feedback regimes, even in the presence of significant ($\geq 1 \mu\text{m}$) bar smile. We also discuss the potential influence of ELOD designs on reliable output power and options for further performance improvement.

Keywords: diode laser, high power, narrow far field, volume holographic grating, frequency stabilization, bar smile insensitivity, high efficiency

1. INTRODUCTION

Diode lasers convert electrical input energy into useful optical output at the highest efficiencies. GaAs-based broad-area diode lasers (BA lasers) with operating wavelength in the $\lambda = 900\text{-}1000$ nm range show the best performance, and devices with stripe width $W = 90\text{...}100 \mu\text{m}$ deliver reliable optical output power, $P_{\text{out}} = 10\text{...}15$ W, with a power conversion efficiency at the operating power, $\eta_E(P_{\text{out}})$, in the range $\eta_E(10\text{...}12 \text{ W}) = 60\text{...}65\%$ (see [1] for a recent review). Such diode lasers are in wide use in material processing applications, either directly [2], or as pump sources for other solid state gain media [3-6]. When used directly, very high overall system efficiency is achieved, at low system cost [2]. Spectral beam combining techniques are used for power scaling in many direct diode systems, where the output of many diode lasers is directed to the work surface via spectrally selective elements (filters, gratings) for maximum power density [2,7-11].

* paul.crump@fbh-berlin.de; www.fbh-berlin.de

When no special measures are taken, the optical output power produced by BA lasers has a relatively broad spectrum, whose integrated spectral width with 95% power content, $\Delta\lambda_{95\%}$, reaches $\Delta\lambda_{95\%} \sim 5\text{-}6$ nm in normal operation [12]. In addition, the wavelength shifts with temperature at a rate of $\delta\lambda/\delta T \sim 0.34$ nm/K, which leads to ~ 10 nm wavelength shift between threshold and P_{out} (due to thermal resistance $R_{\text{th}} > 0$ and $\eta_E < 100\%$). A spectral combining system based on conventional BA lasers therefore has a minimum wavelength spacing between channels of $\sim 15\text{-}20$ nm, limiting power scaling. Spectral stabilization of BA lasers reduces both $\Delta\lambda_{95\%}$ and $\delta\lambda/\delta T$ so is therefore preferred for wavelength-based power scaling. BA lasers stabilized using internal distributed Bragg gratings have recently demonstrated reliable powers and efficiencies ($\eta_E = 58\%$ at $P_{\text{out}} = 10$ W [13,14]) close to that of un-stabilized devices, and reduce the channel spacing to < 2 nm, due to their narrow spectrum and reduced temperature sensitivity ($\Delta\lambda_{95\%} < 1$ nm and $\delta\lambda/\delta T \sim 0.08$ nm/K [13,14]). Wavelength stabilization of BA lasers using external gratings is also in wide use [7-11,15-21], and extremely narrow, highly temperature stable spectra are possible, even in high power systems (a linewidth of < 100 GHz and $\delta\lambda/\delta T < 0.01$ nm/K have been demonstrated). Such narrow, stable spectra are needed (for example) for pumping narrow lines in Alkali-laser systems (see [16,19] and references within). However, external spectral stabilization adds system complexity and hence cost, reduces efficiency and power and can lead to lower reliable power levels [10,20]. In general, the more stringently controlled the wavelength, the larger the performance penalty. When BA lasers are stabilized with external volume holographic gratings (VHGs, also termed VBGs, for volume Bragg gratings) with moderate feedback, the typical reported spectral width lies in the range $\Delta\lambda_{95\%} = 0.5 \dots 1.2$ nm with a power loss of 5-10%, as compared to reference un-stabilized devices.

Most studies of external wavelength stabilization are performed using standard commercial BA lasers, which operate with similar specifications, and set the ultimate limit to system performance. Improvements in BA lasers are therefore sought. We present here a summary of recent studies performed at the Ferdinand-Braun-Institut on BA lasers that have been specifically optimized for wavelength stabilization with external VHGs. These devices are termed throughout ELOD lasers, as they operate with **extremely low vertical divergence**, whilst sustaining high efficiency and high reliable powers [12,21-23]. These ELOD designs were developed within the project SpektraLas, a part of the German national development program "INLAS", and their assessment for use in spectral beam combining systems is planned as part of the recently started EU program BRIDLE¹.

The article is constructed as follows. Firstly, we review the anticipated system benefits of diode lasers with narrow divergence, illustrated by calculations of the coupling efficiency into an optical fiber. Secondly, we present the design approach used, showing how novel active region designs with low-index quantum barriers can enable both high η_E and low vertical far field, $\Theta_V^{95\%}$ (with 95% power content). The un-stabilized performance of the resulting ELOD lasers is then compared to reference devices, and we discuss how they can be further improved. Thirdly, we assess the benefits of ELOD designs on spectral locking range, for the case of slow- and fast-axis collimated laser bars with a VHG placed in the collimated beam. We confirm that bars constructed using ELOD designs operate with increased wavelength locking range and reduced sensitivity to smile. Next, the trade-off between facet reflectivity and grating strength is discussed, again for the case of a VHG located in the collimated beam. Low-smile ELOD and reference bars show comparable power loss for a given feedback, as expected. However, ELOD bars show improved wavelength locking range, enabling the use of weaker VHGs, as preferred for maximum η_E and highest reliable P_{out} . Finally, we discuss the impact of optical feedback on bar reliability, and present initial reliability tests on wavelength stabilized ELOD and reference bars, before concluding.

2. DESIGN CONSIDERATIONS

2.1 Benefit of ELOD diode laser designs for spectrally stabilized systems

BA lasers can be spectrally stabilized with external gratings in many different configurations, as reviewed recently in [18]. However, most high power BA laser are locked using a coupling scheme similar to that shown in Figure 1. A diode laser single emitter or bar is prepared with a high reflection coating ($> 95\%$) on the rear facet and a low reflectivity coating on the front facet (0...5%). The divergent output is collimated first using a fast-axis (vertical) collimation (FAC) lens, followed by a slow axis (in-plane) collimation lens (lens array for bars). A grating is then located in the collimated beam, illustrated schematically in Fig. 1 with a VHG. Spectrally narrow feedback from the VHG is then imaged back

¹ Details of the SpektraLas and BRIDLE programs can be found at the links: <http://www.ot-inlas.de/en/spektralas/> and <http://www.bridle.eu/> respectively.

onto the output facet of the laser bar with a magnification of -1. The overall optical output of the spectrally stabilized BA laser is then typically focused via an additional lens into an optical fiber for beam delivery. Optical losses in such an anamorphic lens system are a combined function of the beam quality and far field angle in both fast and slow axes, as well as the characteristics of the focusing optics and the fiber. Even for the case of diffraction-limited emission in slow and fast axes and ideal optical elements, when the emission angles are large, skew rays are produced, which cannot be effectively coupled into a target of finite NA and finite aperture, leading to optical losses. This is equally true for coupling of the transmitted light from the VHG into an optical fiber and for feedback from the VHG into the diode laser for frequency stabilization. Non-diffraction limited output, non-ideal optics and non-zero alignment tolerance will compound the effect. However, the overall optical loss is a detailed function of the system used. It should also be noted that a narrow far field in the vertical (fast) axis leads to greater tolerance of wide angles in the slow axis, and vice versa. For a fixed optical system, standard design parameters include the feedback strength and spectral width of the grating and the reflectivity of the output facet of the laser.

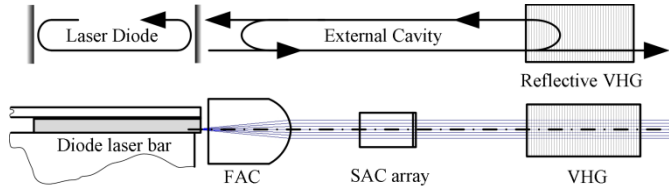


Figure 1: Top: generalized schematic of a diode laser with spectral stabilization in an external cavity configuration. Arrows indicate the optical round-trip and the out-coupling. Bottom: Vertical cross-section of a typical packaging configuration. Emission from the diode laser bar (on heat-sink) is collimated in slow and fast axes, with a VHG in the collimated beam. A spectrally-narrow image of the near-field of the diode laser is directed back to the output facet with a magnification of ≈ -1 .

BA lasers with narrow vertical far fields offer several advantages in such an anamorphic optical system. Firstly, narrower far field angles require lenses with lower numerical aperture, NA (smaller acceptance angle), which are less demanding to manufacture, and simpler to align, lowering costs. Secondly, the proportion of emission into high angle skew-rays is reduced, lowering optical losses. Thirdly, the small emission angle is enabled by using diode lasers with a large vertical waveguide (see section 2.2 for more discussion), meaning that the back-focused image can be more easily matched to the vertical near field, for high coupling efficiency. Good matching of the output and input beams at the laser facet is also essential to prevent performance and reliability hazards: if (for example) the back-coupled beam is focused onto the solder layer, this will be heated and could initiate device failure. Large vertical near fields have a further advantage: when laser bars are soldered onto a heat-sink, some mechanical deformation is always induced, leading to small differences between emitters within the bar in vertical position and pointing angle, collectively termed bar smile. When the vertical near field is significantly larger than the bar smile, losses will be minimized [21]. Finally, designs with narrow vertical far fields can enable high performance in novel wavelength stabilization configurations. For example, VHGs can be located in the un-collimated beam, simplifying the optical design (in this case, narrow far fields have been demonstrated to substantially improve both optical loss and locking range [21].)

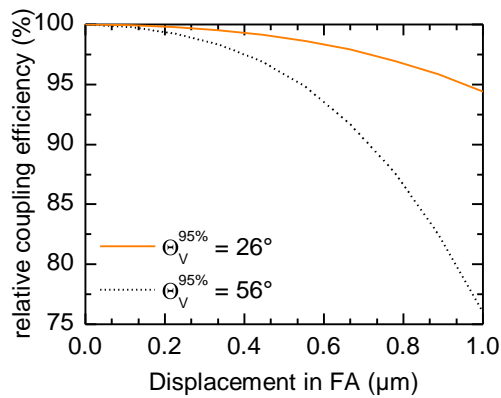


Figure 2: Calculated relative change in fiber coupling efficiency (105 μm core, NA = 0.15) as a function of displacement of the fast-axis collimation lens. Results are presented for diode laser designs with a vertical divergence angle of $\Theta_V^{95\%} = 26^\circ$ (solid line) and $\Theta_V^{95\%} = 56^\circ$ (dashed line).

We illustrate here the expected benefit of narrow vertical far fields on fiber coupling efficiency for a diode laser module based on single emitters with a stripe width, $W = 90 \mu\text{m}$. Calculations were performed for BA lasers with a narrow vertical far field ($\Theta_V^{95\%} = 26^\circ$, $M^2 < 1.2$) and for BA lasers with a typical commercial specification ($\Theta_V^{95\%} = 56^\circ$, $M^2 < 1.2$) that are coupled into a $105 \mu\text{m}$ fiber (NA = 0.15), following techniques described in [24]. In the lateral direction, a beam quality of $M^2 = 16\dots 20$ was used for the calculation, corresponding to operation of single emitters at high bias levels ($> 10 \text{ W}$ per stripe). Matched FAC lenses were used, with an effective focal length of $1100 \mu\text{m}$ and $600 \mu\text{m}$ for the narrow far field and “typical commercial” cases respectively. For the case of ideal alignment, the total optical coupling efficiency was estimated to be 90% for the narrow far field case and 86% for the typical commercial lasers (including Fresnel losses). With manufacturing tolerances, some misalignment is inevitable, and, as an example, Figure 2 shows how vertical misalignment of the FAC lens affects fiber coupling for the two BA laser types: a FAC-lens offset of $0.5 \mu\text{m}$ would lead to a further 5% of optical loss for a BA laser with typical commercial far field, but just 1% for the reduced far field case (in systems based on laser bars, smile effects will compound these losses).

We therefore estimate that for a typical $0.5 \mu\text{m}$ misalignment, diode lasers with $\Theta_V^{95\%} = 26^\circ$ will show 89% coupling into fiber, compared to 82% for typical commercial reference lasers with $\Theta_V^{95\%} = 56^\circ$. Fiber coupling was later measured and confirmed this expectation, with “ELOC2” devices with $\Theta_V^{95\%} = 26^\circ$ (as described in section 3.1) showing 90% and commercial devices with $\Theta_V^{95\%} = 56^\circ$ showing 79% fiber coupling respectively. Overall, a narrow vertical far field potentially enables significantly more “in-fiber” efficiency. Narrow lateral far field is also beneficial, with high in-fiber efficiencies reported for arrays of BA lasers that have conventional vertical far fields $\Theta_V^{95\%} \sim 50^\circ$ and improved in-plane beam quality $M^2 = 10$ (7° far field, $100 \mu\text{m}$ near field), in a different optical design [6].

To summarize, if BA lasers can be produced with $\Theta_V^{95\%} = 26^\circ$ and $\eta_E(10 \text{ W}) > 55\%$ (within 10% of commercial state-of-the-art material), then these are anticipated to lead to improved “in-fiber” power conversion efficiencies and simpler, lower-cost, higher-reliability wavelength stabilized systems. We show in the next section how this can be achieved.

2.2 Design approach for simultaneous high efficiency and narrow vertical far field

Diode lasers with narrow vertical far fields have been studied for many years by many groups, and various design schemes are possible (see [25-28] and references within). Currently, most high power, high-efficiency GaAs-based diode lasers make use of large optical cavity (LOC) vertical waveguide designs, with a waveguide thickness of around $1 \mu\text{m}$, with quantum wells providing the optical gain. The most natural approach for achieving narrow vertical far field is to simply increase waveguide thickness, although sophisticated designs are needed to suppress lasing in higher order vertical modes [26]. The resulting broadening of the optical mode reduces the modal gain, hence increasing threshold, so typically at least two quantum wells are required for reasonable performance [22]. When no special measures are taken, a waveguide thickness of $> 7\text{-}8 \mu\text{m}$ is found to be necessary for operation with $\Theta_V^{95\%} < 30^\circ$, and this compromises performance strongly, leading to low internal efficiency, η_i and high electrical resistance [25,27].

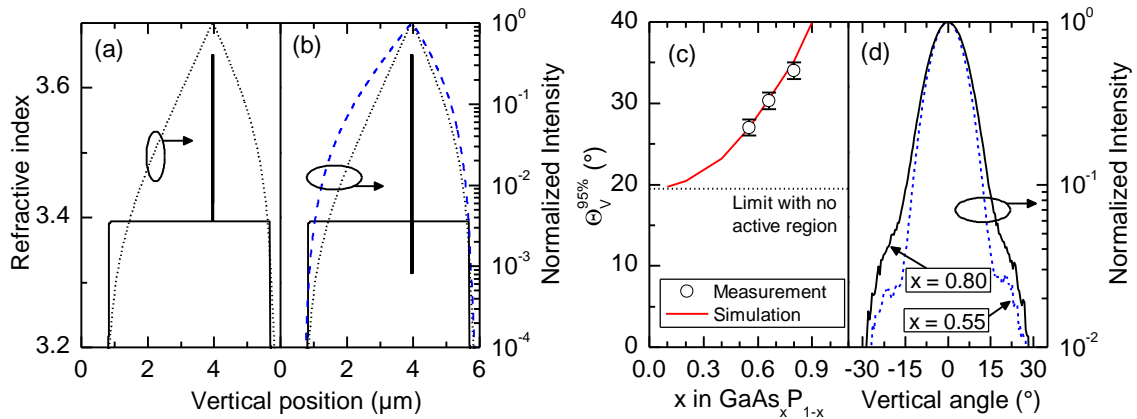


Figure 3: Influence of barrier composition on vertical beam profile. Vertical refractive index profile and resulting calculated optical intensity field of the fundamental mode for (a) conventional GaAs_{0.8}P_{0.2} barriers (dotted line) (b) low-index GaAs_{0.55}P_{0.45} barriers (dashed line), with the near field for GaAs_{0.8}P_{0.2} barriers reproduced for comparison. (c) Vertical far field angle as a function of As-content in the barriers. (d) Measured intensity as a function of vertical angle (far field) for diode lasers with GaAs_{0.8}P_{0.2} barriers (solid line) and GaAs_{0.55}P_{0.45} barriers (dashed line).

One key design challenge is that as the LOC increases in thickness, optical waveguiding due to the active region itself plays an increasing role and sets a lower limit to $\Theta_V^{95\%}$ (the quantum wells have a higher refractive index, n , than the waveguide layer – see Figure 3). Various techniques can be used to compensate for this, for example by coupling to additional vertical waveguides or by using optical trap layers (see Refs. [28-30] and references within). However, these approaches add complexity, increase overall thickness and add hetero-junctions, typically degrading η_E . In the ELOD design presented here, an alternative approach is followed, making use of the barriers between the quantum wells, as discussed in detail in Refs. [22,25]. If the barriers are selected to have lower n than the waveguide layer, they can suppress the active region waveguiding. We illustrate the effect in Figure 3 for a vertical design with using a 4.8 μm thick $\text{Al}_{0.2}\text{Ga}_{0.8}\text{As}$ waveguide, containing three InGaAs quantum wells that provide gain at a wavelength $\lambda = 975$ nm. The wells are separated by $\text{GaAs}_x\text{P}_{1-x}$ barriers where conventionally, $x = 0.8$, and the refractive index of the barriers, n_b is close to that of the waveguide, n_{wg} . When barriers with $x = 0.55$ (for example) are used, then $n_b < n_{\text{wg}}$, and the influence of the active region is suppressed, with simulations showing a broadened vertical near field and narrowed far field. As shown in Figure 3, as x is reduced (phosphor content increased), the far field continues to narrow, as predicted theoretically and confirmed experimentally. We find that for $x = 0.55$, $\Theta_V^{95\%} = 27^\circ$ for a 4.8 μm waveguide, a far field angle that would otherwise require a > 8 μm thick waveguide.

However, the use of low-index quantum barriers has some challenges. Firstly, although high-phosphor GaAsP barriers enable narrow vertical far fields, they also introduce crystal strain, and as phosphor level increases they eventually accumulate material defects, with a practical limit being $x = 0.66$. Secondly, high-phosphor GaAsP barriers have an increased band-gap, which can restrict carrier injection into the active region, potentially suppressing internal efficiency. Figure 4 shows the calculated valence band edge profile near the active region, for light and heavy holes. Conventional $\text{GaAs}_{0.8}\text{P}_{0.2}$ barriers present no injection barrier, with the light hole band edge calculated as having an energy offset from the waveguide, $\Delta E_{\text{LH}} = -44$ meV. In contrast, $\text{GaAs}_{0.55}\text{P}_{0.45}$ barriers lead to $\Delta E_{\text{LH}} = +43$ meV. As noted in [19], the measured internal efficiency remains high ($\eta_i = 93\%$) for both cases. However, when $\Delta E_{\text{LH}} = +70$ meV, degraded performance is observed [25]. Therefore, a practical design limit is $\Delta E_{\text{LH}} \leq 40$ meV. Finally, the introduction of an energy barrier leads also to increases in operation voltage, as noted in [25] and illustrated in Figure 4. The electrical resistance is unchanged, but the turn-on voltage of the diode increases: additional external voltage is required to drive the carriers into the active region. The increase in turn-on voltage is found to scale in a one-to-one relationship with ΔE_{LH} , indicating that hole-injection is responsible. It should be remembered that the voltage increase due to the low-index barriers is substantially lower than the voltage that would be dropped across the > 8 μm thick waveguide necessary to achieve the same far field. To summarize, low index-quantum barriers substantially reduce vertical far field angles, and provided the barrier to hole-injection remains low, their only penalty is a small additional turn-on voltage.

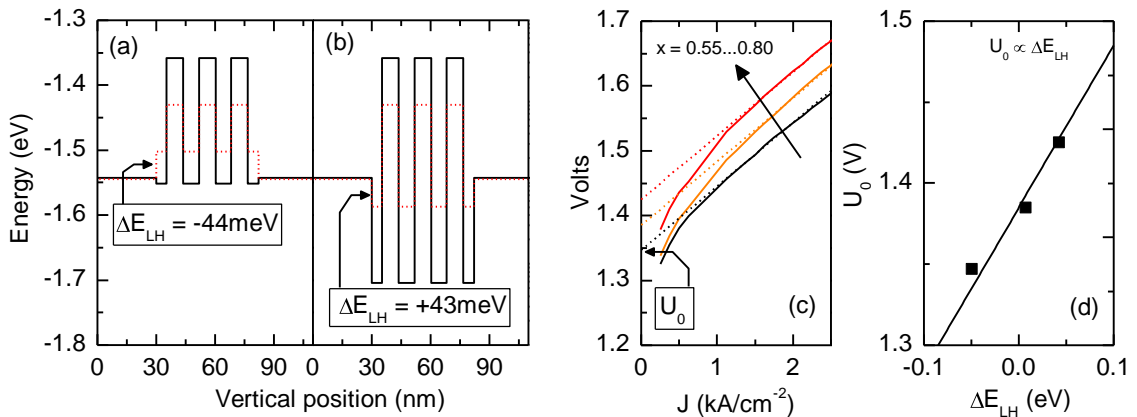


Figure 4: Calculated influence of barrier composition on vertical valence band-edge profile for light holes (dotted line) and heavy holes (solid line) for (a) $\text{GaAs}_{0.8}\text{P}_{0.2}$ barriers and (b) low-index $\text{GaAs}_{0.55}\text{P}_{0.45}$ barriers. The energy difference for light holes between the band edges of the waveguide and the barriers, ΔE_{LH} , is noted. (c) Measured voltage as function of current density for different As-content in the barriers (solid lines). A linear fit (dashed lines) is used to derive turn-on voltage, U_0 . (d) Measured U_0 as a function of calculated ΔE_{LH} (points). A fit line with slope = 1 is shown for comparison (solid line).

3. PERFORMANCE OF ELOD LASERS COMPARED TO REFERENCE DEVICES

3.1 Un-stabilized single emitter performance

Results on two generations of ELOD devices are presented here, ELOD1 (taken from [19]) and ELOD2 (from [20]). ELOD1 devices use a 4.8 μm thick $\text{Al}_{0.2}\text{Ga}_{0.8}\text{As}$ vertical waveguide, with three InGaAs quantum wells, separated by $\text{GaAs}_{0.66}\text{P}_{0.34}$ barriers. Devices were fabricated in high power BA laser format, with cavity length, $L = 3 \text{ mm}$ and $W = 90 \mu\text{m}$, their facets were passivated then coated with front and rear facet reflectivities of $R_f = 0.5\%$ and $R_r = 98\%$ respectively. The devices were subsequently bonded p-side down with hard-solder on CuW carriers and tested in continuous wave (CW) mode at 25°C . The ELOD1 devices operated with $\Theta_v^{95\%} = 30^\circ$, and a reliable output of $P_{\text{out}} = 10 \text{ W}$ was demonstrated, with $\eta_E(10 \text{ W}) = 55\%$.

In order to achieve even narrower vertical far fields, the waveguiding of the active region must be further suppressed. As the index of the barriers could not be further reduced (additional phosphor would initiate material defects), instead the index of the waveguide was increased – achieved by lowering the aluminum content of the waveguide to $\text{Al}_{0.15}\text{Ga}_{0.85}\text{As}$. No other changes were made to the vertical design. The reduced waveguiding from the active region leads to a wider vertical near field and hence the confinement in the quantum wells is reduced, decreasing the modal gain parameter Γg_0 from 29 cm^{-1} to 21 cm^{-1} . A higher front facet coating and longer resonator were necessary to compensate for this lower gain, and diode lasers were fabricated using this new ELOD2 design with $L = 4 \text{ mm}$, $W = 90 \mu\text{m}$, $R_f = 1\%$ and $R_r = 98\%$. The final ELOD2 devices operated with both narrower vertical far field and increased power conversion efficiency, demonstrating $\Theta_v^{95\%} = 26^\circ$, with $\eta_E(10 \text{ W}) = 58\%$, measured under the same test conditions as the ELOD1 lasers.

In order to most clearly demonstrate the performance benefits of the ELOD designs, it is helpful to perform side-by-side measurements on reference devices with conventional vertical far field angles. In previous work, just such a detailed comparison was presented, for ELOD1 devices as described in Ref. [21]. The reference material was also fabricated at the FBH, and is described in [13]. In summary, the reference devices also operated at $\lambda = 975 \text{ nm}$, and the vertical design uses a 2.1 μm thick $\text{Al}_{0.15}\text{Ga}_{0.85}\text{As}$ waveguide that contains a double-quantum well active region. Reference BA lasers were fabricated with $L = 3 \text{ mm}$, $W = 90 \mu\text{m}$, $R_f = 1\%$ and $R_r = 98\%$, and were tested using the same conditions as for the ELOD devices, demonstrating $\Theta_v^{95\%} = 45^\circ$, with $\eta_E(10 \text{ W}) = 65\%$. Figure 5 compares the performance of the ELOD2 and reference devices, and shows that the (calculated) vertical near field with 95% power content, $W_{95\%}$, is increased from $W_{95\%} = 1.6 \mu\text{m}$ for the reference design to $W_{95\%} = 3.0 \mu\text{m}$ for the ELOD2 design, so that bar smile (or vertical misalignment of the FAC lens) of at least $1 \mu\text{m}$ is likely to be tolerated. The $\sim 2\times$ wider vertical near field and $\sim 2\times$ narrower vertical far field of the ELOD2 devices comes at the cost of a 7% reduction in power conversion efficiency, from $\eta_E(10 \text{ W}) = 65\%$ to $\eta_E(10 \text{ W}) = 58\%$. It should be noted that at lower per-emitter power levels, as often used in bar configuration, the efficiency differences are larger, as the devices operate closer to threshold.

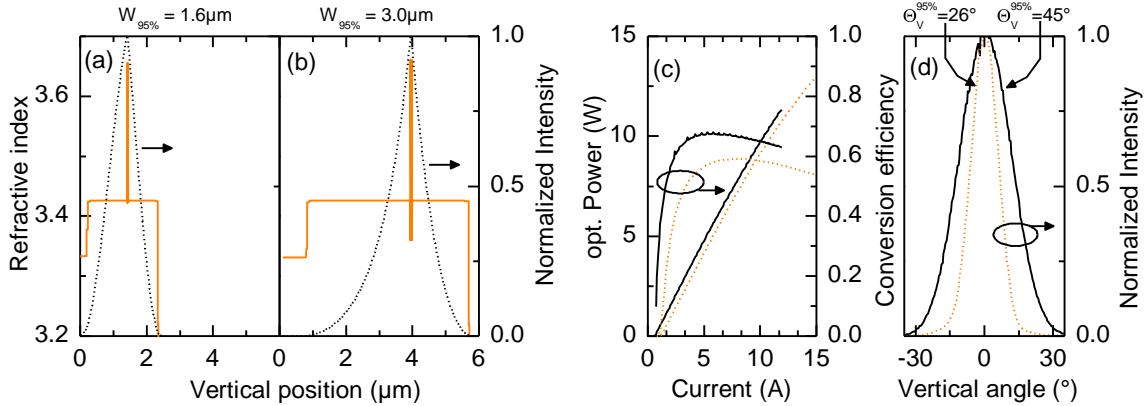


Figure 5: Performance comparison of reference and ELOD2 BA laser single emitters with stripe width $W = 90 \mu\text{m}$. Vertical refractive index profile and resulting calculated intensity profile of the fundamental mode for (a) reference devices and (b) ELOD2 devices. The calculated mode size with 95% power content is noted. (c) 25°C CW measured optical output power and power conversion efficiency as function of current for reference (solid line) and ELOD2 BA lasers (dashed line). (d) Measured optical output as a function of vertical angle (far field) for reference and ELOD2 BA lasers.

3.2 BA laser bar spectral stabilization performance in the presence of smile, for a fixed VHG design

Although high efficiencies and powers are observed from free-running ELOD devices, high performance is also required when they are spectrally stabilized. Here, we compare spectrally stabilized reference, ELOD1 and ELOD2 BA laser bars. Each bar is 1 cm wide, and contains 19 emitters identical to those described in section 3.1. The bars have an emitter-to-emitter pitch of 500 μm , and are mounted junction-side down with indium solder onto a final package. Reference and ELOD1 bars are attached to 2.5 cm-square passively cooled carriers, termed CCP (or CS) mounts, and have a front facet coating close to 1%. In contrast, ELOD2 bars are mounted on a micro-channel cooler and have a very low reflectivity facet coating of $R_f < 0.1\%$. The tested devices showed peak-to-valley smile values of in the range of 0.8 to 2 μm (measured after collimation). Without the feedback of the external resonator, the centroid wavelength of the integrated bar spectrum (to a good approximation) varies linearly with current above threshold at a rate ξ , due to the shift of material gain wavelength with active region temperature. ξ depends on the thermal resistance and therefore on the packaging of the diode laser bars. Measured values are $\xi_{\text{Ref}} = 0.11 \text{ nm/A}$, $\xi_{\text{ELOD1}} = 0.12 \text{ nm/A}$ and $\xi_{\text{ELOD2}} = 0.09 \text{ nm/A}$ for reference, ELOD1 and ELOD2 bars respectively (ELOD2 bars vary more slowly, due to their improved cooling). FAC and SAC collimation lenses and a VHG were subsequently introduced, which were adapted to the laser design so that the divergence of the collimated beam and therefore the feedback of the diffraction grating was the same for all tested bars. The optical characteristics of the measured bars and their collimation lenses are summarized in Table 1. The measured smile error of each bar (after collimation) is shown in Figure 6, determined by imaging the collimated beam into a high resolution camera.

The stabilization range has been investigated using an imaging external resonator with image reversal, as shown in Figure 1. VHGs that supply low feedback were investigated, to most clearly demonstrate the benefit of narrow vertical far field. Specifically, the VHGs had maximum diffraction efficiencies of $8\% \leq \eta_{\text{max}} \leq 10\%$, and were fine-adjusted in the collimated beam of three diode laser bars under test (Table 1) with the primary objective of maximizing the stabilization range. Here, we define a diode laser bar as being spectrally stabilized when 90% of the emitted power is included in a narrow spectral range $2\delta\lambda = 1.2 \text{ nm}$ around the Bragg wavelength λ_B of the VHG, following Equation 1. Subsequently, a stabilization range, $\Delta\lambda^{(S)}$, is calculated, defined as the maximum offset between the gain wavelength and λ_B where $2\delta\lambda$ remains $\leq 1.2 \text{ nm}$.

$$\frac{\int_{\lambda_B - \delta\lambda}^{\lambda_B + \delta\lambda} I(\lambda)}{\int_0^{\infty} I(\lambda)} > 0.9 \quad (1)$$

	Reference	ELOD1	ELOD2
Resonator length [mm]	3	3	4
Facet AR coat [%]	0.7	1.2	< 0.1
FAC focal length [μm]	1200	1500	1500
SAC focal length [μm]	2600	2600	2600
Smile PV after collimation [μm]	1.1	0.8	2.0
Vertical mode size, $W_{95\%}$ [μm]	1.6	2.7	3.0

Table 1: Characteristic data of the diode laser bars and optical system under test

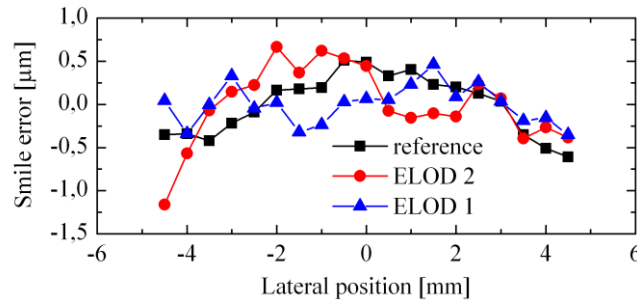


Figure 6: Measured smile error of the diode laser bars designs under study (measured after the collimation optics).

Firstly, in this weak feedback regime, the reference bars are found to lock very poorly, as seen in Figure 7, and the spectral bandwidth of the reference structure never falls below 1.2 nm, leading to $\Delta\lambda_{\text{Ref}}^{(S)} \approx 0$ nm. In contrast, the ELOD1 bar shows improved stabilization bandwidth, $\Delta\lambda_{\text{ELOD1}}^{(S)} = 4.6$ nm (corresponding to a current locking range of $\Delta I_{\text{ELOD1}} = 40$ A), also shown in Figure 7. As shown experimentally in Ref. [21], the difference in locking performance is due to the smile error. The emitters in the reference bars have a maximum mechanical offset of $1.1 \mu\text{m}$, close to the vertical near-field size ($W_{95\%} = 1.6 \mu\text{m}$). This means that the reverse image from the VHG cannot be effectively delivered to all emitters, and some will not be stabilized. In contrast, the $0.8 \mu\text{m}$ smile for the ELOD1 bar is only 1/3 of its vertical near field size, and all emitters are spectrally stabilized. Hence, the main influence on the spectral stabilization bandwidth is the smile error.

The ELOD2 diode laser bar operates with substantially improved performance, and is stabilized from threshold current = 20 A up to $I \geq 160$ A, due in part to its low front facet reflectivity and improved cooling. The stabilization bandwidth is $\Delta\lambda_{\text{ELOD2}}^{(S)} \geq 12.7$ nm ($\Delta I_{\text{ELOD2}} \geq 140$ A). Although the absolute smile error of the ELOD-2 diode laser bar is the largest among the tested bars at $2 \mu\text{m}$, this is lower than the mode size and all of the 19 emitters are stabilized. We therefore conclude that ELOD designs lead to improved locking range and lower smile sensitivity in BA laser bars, potentially allowing lower strength VHGs and high-smile hard-solder packaging to be used, for maximum reliability and system robustness.

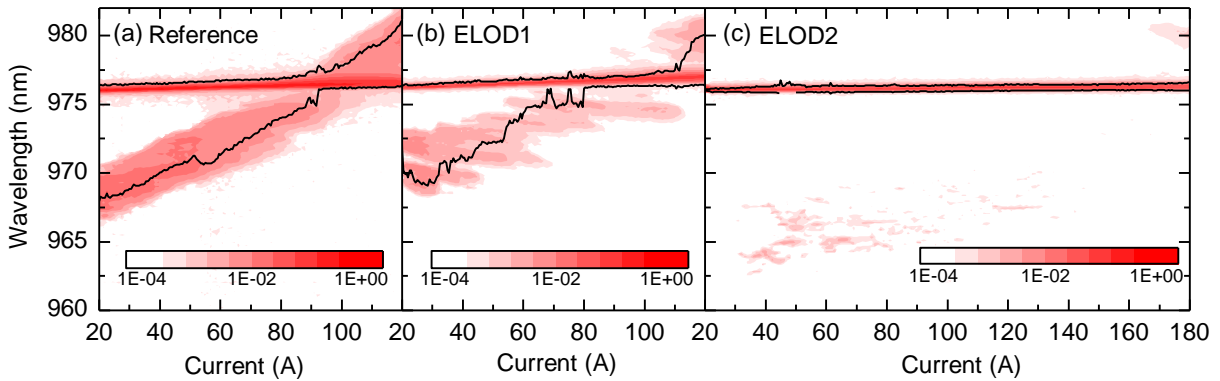


Figure 7: Wavelength as a function of injection current for VHG stabilized BA laser bars, with normalized, integrated optical intensity presented as a logarithmically scaled false-color plot. The 90% power level limit to the spectrum is marked in each graph (solid lines). Results are shown for (a) reference material mounted on a CCP, (b) ELOD-1 material mounted on a CCP and (c) ELOD-2 material mounted on a micro-channel cooler.

3.3 Low-smile BA laser bar spectral-stabilization performance, as a function of facet and VHG feedback level

Section 2.1 showed that narrow vertical far field minimizes power losses due to misalignment of optics and in section 3.2, we also demonstrated how ELOD-based designs improve stabilization performance for bars with significant smile ($\sim 1 \mu\text{m}$ or higher). However, not all bars show high smile, and a carefully optimized soldering process can consistently produce bars with smile of $< 0.4 \mu\text{m}$, especially for low temperature solders (e.g. indium). Also, as alignment tools improve, the losses associated with misalignment will fall. Here, we show experimentally how BA laser bars using ELOD designs operate with improved spectral stabilization, even for bars with smile $< 0.4 \mu\text{m}$ and precision-aligned optics. We assess reference and ELOD2 bars, as described in sections 3.1 and 3.2, stabilized as in Figure 1, mounted on CCP with indium solder and tested in CW mode at 25°C . The use of indium solder restricts the maximum useable current level to 70A, corresponding to a current per emitter of 3.7 A. As can be seen from Figure 5, these currents are significantly below peak efficiency, and threshold current will play a key role in limiting output power. The FAC, SAC and VHG alignment was performed on an optical table, for optimal precision.

A detailed comparison of the spectral stabilization of low-smile, precision aligned reference and ELOD2 bars has therefore been performed as a function of the reflectivity of the volume holographic grating and the front facet reflectivity. To this end, we have examined five different front facet reflectivities, covering the range from $R_f < 0.05\%$ up to 5%, in combination with two different VHG-reflectivities of $R_{\text{VHG}} = 15\%$ and 20% , respectively (reference bars were only available with two front facet coating levels, of $R_f = 0.5\%$ and 2%). As a first step, Figure 8 presents the influence of R_f and R_{VHG} on the integrated optical output power at the maximum CW bar current of 70 A. The power

emitted by un-stabilized bars is a strong function of R_f , whose form is most clearly demonstrated for the ELOD2 design. At the lowest front facet reflectivity ($R_f < 0.1\%$) the feedback from the front facet is small, leading to a high bar threshold current of about 40 A, reducing power and efficiency. The power increases with R_f , due to threshold current being reduced, and is maximized for $R_f = 2\%$, where bar threshold is 20 A. For front facet reflectivity above 2%, threshold current plays a smaller role, and optical output power is reduced due to lower slope. The reference bars have a smaller transparency current density ($J_{\text{transp}} = 151 \text{ A/cm}^2$ compared to $J_{\text{transp}} = 220 \text{ A/cm}^2$ for the ELOD2 design), and comparable modal gain parameter ($\Gamma_{g_0} = 21 \text{ cm}^{-1}$ for both reference and ELOD2) which means lower values of R_f can be used before threshold becomes excessive. Lower R_f leads to increased slope, increasing power, due to the larger out-coupling. Therefore, for the reference bars, peak power is seen at lower $R_f = 0.5\%$, where bar threshold is 10 A. We anticipate lower powers for the reference bars if R_f were reduced to $< 0.5\%$.

Figure 8 also shows how the output power at 70 A varies when the bars are stabilized using VHGs with reflectivity of $R_{\text{VHG}} = 15\%$ and 20% . For reference lasers with $R_f = 0.5\% \dots 2\%$ and ELOD2 bars with $R_f = 1 \dots 5\%$, overall output power decreases as R_{VHG} is increased, dropping $\sim 4\%$ for $R_{\text{VHG}} = 15\%$ and $\sim 10\%$ for $R_{\text{VHG}} = 20\%$. Following section 2.1, the observation of similar power loss levels independent of vertical far field angle indicates that reference and ELOD2 bars are aligned to good precision. When ELOD2 bars are prepared with $R_f < 1\%$, VHG stabilization helps reduce threshold current, compensating for some of the additional power loss in this low-current-per-emitter regime. Overall, the highest overall stabilized powers and efficiencies are achieved when the most efficient un-stabilized bars are used; that is to say, reference bars with $R_f = 0.5\%$ and ELOD2 bars with $R_f = 2\%$ also show the highest powers and hence efficiencies after stabilization. The light-current curves for the highest efficiency configuration are compared in Figure 9, namely reference ($R_f = 0.5\%$) and ELOD2 ($R_f = 2\%$), with and without stabilization using a VHG with $R_{\text{VHG}} = 15\%$. As noted above, the ELOD2 bar has a threshold of 20 A, double that of the reference bar, and threshold is minimally affected by stabilization. Both bars have similar slopes (close to 1 W/A), which are reduced $\sim 4\%$ after VHG stabilization.

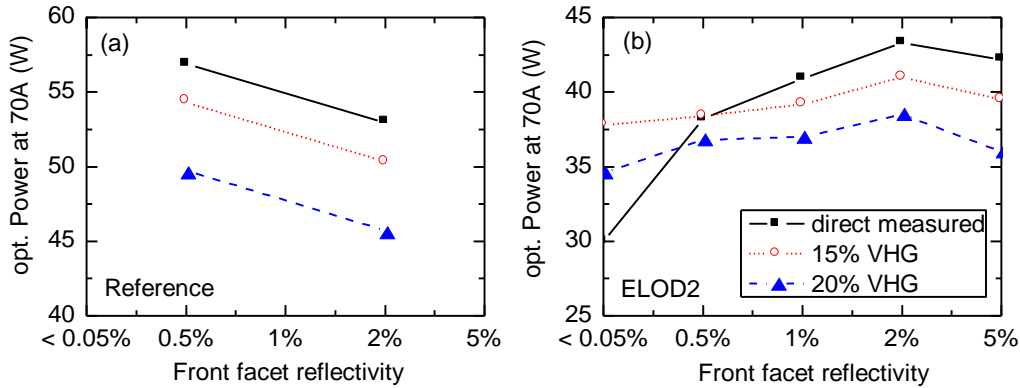


Figure 8: Optical output power per bar (CW 25°C) at a drive current of 70 A as a function of front facet reflectivity for spectrally un-stabilized bars (squares), and for bars stabilized using a VHG with $R_{\text{VHG}} = 15\%$ (circles) and $R_{\text{VHG}} = 20\%$ (triangles). Results are presented for (a) reference and (b) ELOD2 bars.

Although low power loss is important for high overall efficiencies, the bars must operate with narrow, stable spectra to be useable in spectral beam combining applications. Firstly, every ELOD2 bar investigated was fully locked from 30 A to 70 A for all R_f and R_{VHG} values investigated, with no side peaks and spectral widths $2\delta\lambda \sim 0.5 \text{ nm}$. Lower R_{VHG} values are anticipated to also show good wavelength locking, and reduced power losses. This was not the case for the reference bars, which developed 5% intensity class side peaks for $R_{\text{VHG}} = 15\%$, as illustrated in Figure 9. Therefore, reference bars require $R_{\text{VHG}} = 20\%$ for high locking performance, which bring an additional optical loss and are a higher reliability risk, as more light is directed onto the facet. The additional losses from the VHG effectively cancel the efficiency benefit of the reference design over the ELOD2 design, especially when these are operated at the 7-10 W per-emitter power level. Therefore, although low smile bars and maximum precision alignment of the optics was used, the ELOD2 bars continue to show improved stabilization performance.

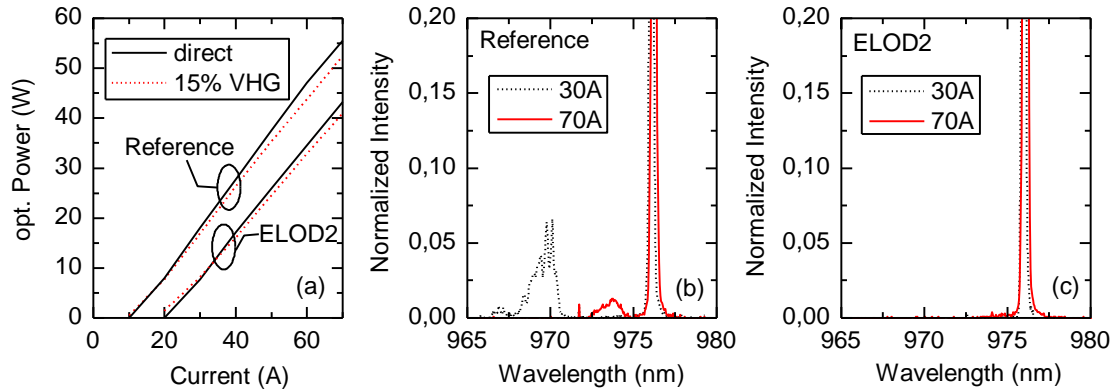


Figure 9: Performance of low smile reference and ELOD2 laser bars, with and without spectral stabilization. (a) Output power as a function of current for a reference ($R_f = 0.5\%$) and an ELOD2 ($R_f = 2\%$) diode laser bar, with (dashed line) and without (solid line) wavelength stabilization by means of a VHG with $R_{VHG} = 15\%$. (b) Normalized integrated optical output power as a function of wavelength (spectrum) for the reference bar, VHG stabilized. Intensity is shown scaled to 20% level, to more clearly reveal the side peaks. (c) Spectrum of the wavelength stabilized ELOD2 bar.

3.4 Reliability assessment

Several authors have noted lower per-emitter failure powers and reduced reliable power levels when BA lasers are wavelength stabilized using VHG's [10,20]. As discussed earlier, ELOD designs with wide vertical near fields are potentially less sensitive to these failure mechanisms. We have therefore compared the aging performance of ELOD1 and reference bars, prepared with $R_f = 1.3\%$ and $R_f = 0.8\%$ respectively. The bars contain 19 emitters, are mounted junction side down on CCP packages with indium solder, with smile of $< 1\ \mu\text{m}$, and they are wavelength stabilized using the configuration shown in Figure 1. A relatively weak VHG was used, with $R_{VHG} \sim 7\%$ and the resulting spectra are comparable to those shown in Figures 7(a) and 7(b). Three reference and three ELOD1 bars were aged in constant CW power mode, firstly at 40 W per bar, which was then stepped up to 45 W per bar, as shown in Figure 10. The CCP temperature is regulated to 25°C . The use of indium solder limited the peak aging current to $\sim 70\ \text{A}$, so bar powers $> 45\ \text{W}$ are not assessed. The aging conditions are a “best case” for VHG stabilization, due to the low smile and low feedback levels. To date, all bars assessed operate failure free, with no indication of earlier degradation in the reference bars, with the ELOD bars requiring $\sim 10\ \text{A}$ increased drive current due to their $\sim 10\ \text{A}$ higher threshold current. Further updates will be reported in future publications.

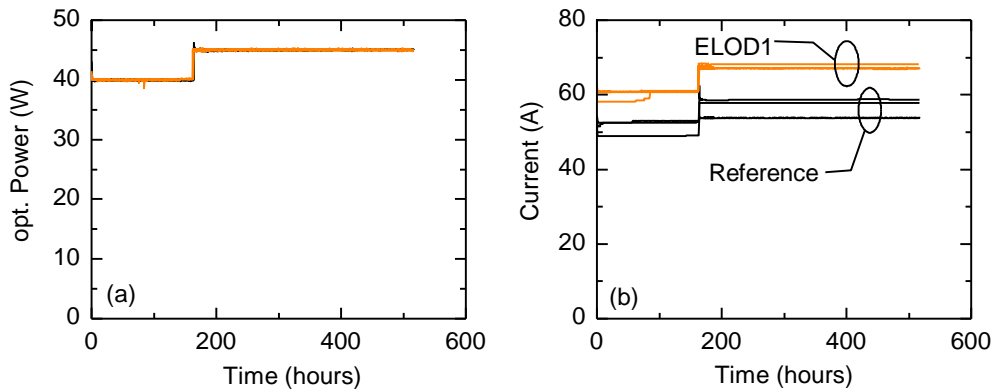


Figure 10: Initial 25°C CW reliability assessment of low-smile reference ($R_f = 0.8\%$) and ELOD1 ($R_f = 1.3\%$) laser bars, spectrally stabilized by means of VHG's with $R_{VHG} = 7\%$. (a) Output power as a function of time. (b) Operation current as a function of time.

4. CONCLUSIONS AND NEXT STEPS

Efficient, high power spectrally stabilized BA lasers are under intensive development, being needed both for power scaling in direct-diode material processing tools via spectral-beam-combining as well as for pumping of narrow lines in solid-state, gas and fiber lasers. External spectral stabilization using volume holographic gratings leads to the narrowest and most temperature stable spectra, but also increases assembly cost and reduces power conversion efficiency, and the necessary back reflection introduces reliability hazards. Most development to date has been performed using standard commercial diode lasers with a vertical far field angle $\Theta_V^{95\%} = 45\dots55^\circ$ range (95% power content), with a vertical near field of $W_{95\%} \sim 1 \mu\text{m}$. We have shown that newly developed 975 nm BA lasers with **extremely low vertical divergence** of $\Theta_V^{95\%} = 26^\circ$ and wide vertical near field of $W_{95\%} = 3.0 \mu\text{m}$ (ELOD designs) offer many performance advantages. First, the ELOD design process and device performance was presented, showing how the use of low index quantum barriers suppresses optical waveguiding from the active region, enabling narrower far field to be achieved with thinner vertical waveguides than would otherwise be possible, for reduced electrical resistance and consequently higher power conversion efficiency. We showed how “second-generation” ELOD2 single emitters with $90 \mu\text{m}$ stripe width operate with power conversion efficiency at 10 W CW output $\eta_E(10 \text{ W}) = 58\%$, just 7% reduced from reference devices with $\eta_E(10 \text{ W}) = 65\%$ and $\Theta_V^{95\%} = 45^\circ$ and $W_{95\%} = 1.6 \mu\text{m}$.

The demonstrated benefits of ELOD designs for spectral stabilization using VHGs were as follows. Firstly, when BA lasers are spectrally stabilized in the collimated regime (VHG located after fast- and slow-axis collimation lenses), the reduced vertical far field angle of the ELOD devices leads to much greater alignment tolerances and lower coupling loss into fiber. For example, a $\sim 5\times$ reduction in the power loss due to any misalignment of the fast-axis lens was calculated. Secondly, the wide vertical near field of ELOD designs was shown to reduce the sensitivity of spectral stabilization to any mechanical deformation (smile) introduced when soldering BA laser bars onto heat-sinks, with side-mode free operation seen even for bars with $2 \mu\text{m}$ of smile and weak feedback ($R_{\text{VHG}} = 8\dots10\%$). Thirdly, even for the case of low smile ($< 0.4 \mu\text{m}$) soldering and precise (benchtop) optical alignment, ELOD bars were shown to deliver improved stabilization performance compared to reference bars, with side-mode free spectra sustained to lower VHG feedback levels. We showed that $R_{\text{VHG}} \leq 15\%$ is required for ELOD bars, corresponding to power losses of $< 4\%$, compared to $R_{\text{VHG}} \geq 20\%$ for reference material, corresponding to power losses of $> 10\%$. Finally, the improved alignment tolerance, wider vertical near fields and lower necessary feedback levels for the ELOD designs are anticipated to lead to higher reliable power levels, with initial reliability data presented. Overall, ELOD BA lasers are expected to deliver comparable or higher “in-fiber” efficiencies to reference designs, with greatly improved alignment tolerances, and higher reliable powers.

Building on these studies, further increased ELOD efficiency and power may be achievable by using thinner vertical structures, enabled by improved suppression of the waveguiding from the active region. For example, if AlGaAs were used as a barrier layer, this has a refractive index that can be varied over a wider range without introducing significant crystal strain, for more design freedom. This is likely to be particularly important when ELOD designs are transferred to shorter wavelengths, where AlGaAs waveguides with higher aluminum content and lower refractive index are required, limiting the impact of the GaAsP-barriers. Secondly, improved system performance based on existing ELOD designs is anticipated when low-smile bars are combined with intermediate strength VHGs, with $R_{\text{VHG}} \sim 10\%$. Finally, the benefit of ELOD-based designs in real spectral-beam-combining systems will be assessed as part of the BRIDLE program [31], and reported in later publications. In summary, efficiency optimized diode laser designs with extremely low vertical divergence are anticipated to play an important role in future high power laser systems.

5. ACKNOWLEDGEMENTS

This work was supported in part by the German Federal Ministry of Education and Research project SpektraLAS (part of the INLAS program) under Contracts 13N9730 (FBH), 13N9729 (ILT) and 13N9725 (DILAS). Support from the European Commission as part of the BRIDLE program (a Framework 7 project, Contract 314719) is also gratefully acknowledged.

The authors thank Bernd Sumpf and Sabine Ullrich for extensive assistance with the reliability studies.

4. REFERENCES

- [1] Crump, P. Erbert, G., Wenzel, H., Frevert, C., Schultz, C. M., Hasler, K-H., Staske, R., Sumpf, B., Maaßdorf, A., Bugge, F., Knigge, S. and Tränkle, G., "Efficient High-Power Laser Diodes," Accepted for publication in *IEEE J. Sel. Top. Quantum Electron.*, (2013).
- [2] Strohmaier, S., An, H. and Vethake, T., "Industrial High Power Diode Lasers: Reliability, Power and Brightness," *Proc. SPIE 8241, 82410Z* (2012).
- [3] Yu, H., Kliner, D. A. V., Liao, K-H., Segall, J., Muendel, M. H., Morehead, J. J., Shen, J., Kutsuris, M., Luu, J., Franke, J., Nguyen, K., Woods, D., Vance, F., Vecht, D., Meng, D., Duesterberg, R., Xu, L., Skidmore, J., Peters, M., Guerin, N., Guo, J., Cheng, J., Du, J., Johnson, B., Yin, D., Hsieh, A., Cheng, P., Demir, A., Cai, J., Gurram, R., Lee, K-W., Raju, R., Zou, D., Srinivasan, R., Saini, M., Zavala, L., Rossin, V., Zucker, E. P., Ishiguro, H. and Sako, H., "1.2-kW single-mode fiber laser based on 100-W high-brightness pump diodes," *Proc. SPIE 8237, 82370G* (2012).
- [4] Langner, A., Such, M., Schötz, G., Just, F., Leich, M., Schwuchow, A., Grimm, S., Zimer, H., Kozak, M., Wedel, B., Rehmann, G., Bachert, C. and Krause, V., "Multi-kW single fiber laser based on an extra large mode area fiber design," *Proc. SPIE 8237, 82370F* (2012).
- [5] Matthews, D. G., Kleine, K., Krause, V., Koesters, A., Duennwald, D. and Pflueger, S., "A 15 kW Fiber-Coupled Diode Laser for Pumping Applications," *Proc. SPIE 8241, 824103* (2012).
- [6] Köhler, B., Ahlert, S., Bayer, A., Kissel, H., Müntz, H., Noeske, A., Rotter, K., Segref, A., Stoiber, M., Unger, A., Wolf, P. and Biesenbach, J., "Scalable high-power and high-brightness fiber coupled diode laser devices," *Proc. SPIE 8241, 824108* (2012).
- [7] Fan, T. Y., "Laser Beam Combining for High-Power, High-Radiance Sources," *IEEE J. Sel. Top. Quant. Electron.* 11(3), 567-577 (2005).
- [8] Andrusyak, O., Smirnov, V., Venus, G., Rotar, V. and Glebov, L., "Spectral Combining and Coherent Coupling of Lasers by Volume Bragg Gratings," *IEEE J. Sel. Top. Quant. Electron.* 15(2), 344-353 (2009).
- [9] Huang, R. K., Chann, B., Burgess, J., Kaiman, M., Overman, R., Glenn, J. D. and Tayebati, P., "Direct diode lasers with comparable beam quality to fiber, CO₂, and solid state lasers," *Proc. SPIE 8241, 824102* (2012).
- [10] Heinemann, S., Lewis, B., Michaelis, K. and Schmidt, T., "Very High Brightness Diode Lasers," *Proc. SPIE 8241, 82410L* (2012).
- [11] Grasso, D. M., Shou, N., Chen, H., Pathak, R., Liang, P., Roh, S. D. and Lee, D., "Wavelength-stabilized, fiber-coupled diode laser with 500 W output and 20 mm-mrad beam quality," *Proc. SPIE 8241, 82410K* (2012).
- [12] Crump, P., Schultz, C. M., Pietrzak, A., Knigge, S., Brox, O., Maaßdorf, A., Bugge, F., Wenzel, H. and Erbert, G., "975-nm high-power broad area diode lasers optimized for narrow spectral linewidth applications," *Proc. SPIE 7583, 75830N* (2010).
- [13] Schultz, C.M., Crump, P., Maaßdorf, A., Brox, O., Bugge, F., Mogilatenko, A., Wenzel, H., Knigge, S., Sumpf, B., Weyers, M., Erbert, G. and Tränkle, G., "In situ etched gratings embedded in AlGaAs for efficient high power 970nm distributed feedback broad-area lasers," *Appl. Phys. Lett.* 100, 201115 (2012).
- [14] Crump, P., Schultz, C. M., Wenzel, H., Erbert, G., and Tränkle, G., "Efficiency-optimized monolithic frequency stabilization of high-power diode lasers" *J. Phys. D: Appl. Phys.* 46, 013001 (2012).
- [15] Steckman, G. J., Liu, W., Platz, R., Schroeder, D., Moser, C. and Havermeier, F., "Volume holographic grating wavelength stabilized laser diodes," *IEEE J. Sel. Topics Quantum Electron.* 13(3), 672-678 (2007).
- [16] Gourevitch, A., Venus, G., Smirnov, V., Hostutler, D. A. and Glebov, L., "Continuous wave, 30 W laser-diode bar with 10 GHz linewidth for Rb laser pumping," *Optics Lett* 33(7), 702-704 (2008).
- [17] Köhler, B., Brand, T., Haag, M., Biesenbach, J., "Wavelength stabilized high-power diode laser modules," *Proc. SPIE.* 7198, 719810 (2009).
- [18] Chi, M., and Petersen, P. M. "Edge emitters with external cavities," *Landolt-Bornstein New Series (Springer-Verlag, Berlin, Germany) Group VIII (Advanced Materials and Technologies: Laser Physics and Applications; Laser Systems) 1 (B)*, 245-257 (2011).
- [19] Kissel, H., Köhler, B., and Biesenbach, J., "High-power diode laser pumps for alkali lasers (DPALs)," *Proc. SPIE 8241, 82410Q* (2012).
- [20] Li, Y., Negoita, V., Barnowski, T., Strohmaier, S. and Treusch, G., "Wavelength Locking of High-Power Diode Laser Bars by Volume Bragg Gratings," *Proc. IEEE Summer Topical Session on High-Power Semiconductor Lasers (Seattle USA), TuA3.2* (2012).

- [21] Crump, P., Hengesbach, S., Witte, U., Hoffmann, H.D., Erbert, G. and Tränkle, G., "High Power Diode Lasers Optimized for Low Loss Smile-insensitive External Spectral Stabilization" *IEEE Photonics Technol. Lett.* 24(8), 703-705 (2012).
- [22] Crump, P., Pietrzak, A., Bugge, F., Wenzel, H., Erbert, G. and Tränkle, G., "975 nm high power diode lasers with high efficiency and narrow vertical far field enabled by low index quantum barriers," *Appl. Phys. Lett.* 96, 131110 (2010).
- [23] Pietrzak, A., Crump, P., Wenzel, H., Bugge, F., Fricke, J. and Erbert, G., "High Power Diode Lasers with Very Narrow Vertical Beam Divergence," *Proc. Photonex 2011 (Coventry UK)*, (2011).
- [24] Hengesbach, S., Witte, U., Traub, M. and Hoffmann, H.D., "Simulation and analysis of volume holographic gratings integrated in collimation optics for wavelength stabilization," *Proc. SPIE 7918*, 79180A (2011).
- [25] Pietrzak, A., Crump, P., Wenzel, H., Erbert, G., Bugge, F. and Tränkle, G., "Combination of Low-Index Quantum Barrier and Super Large Optical Cavity Designs for Ultranarrow Vertical Far-Fields From High-Power Broad-Area Lasers," *IEEE J. Sel. Top. Quantum Electron.* 17(6), 1715-1722 (2011).
- [26] Erbert, G., Bugge, F., Fricke, J., Ressel, P., Staske, R., Sumpf, B., Wenzel, H., Weyers, M. and Tränkle, G., "High-Power High-Efficiency 1150-nm Quantum-Well Laser," *IEEE J. Sel. Top. Quantum Electron.* 11(5), 1217-1222 (2005).
- [27] Bugge, F., Zorn, M., Zeimer, U., Pietrzak, A., Erbert, G. and Weyers, M., "MOVPE growth of InGaAs/GaAsP-MQWs for high-power laser diodes studied by reflectance anisotropy spectroscopy," *J. Cryst. Growth* 311(4), 1065-1069 (2009).
- [28] Malag, A., Jasik, A., Teodorczyk, M., Jagoda, A. and Kozłowska A., "High-Power Low Vertical Beam Divergence 800-nm-Band Double-Barrier-SCH GaAsP-(AlGa)As Laser Diodes," *IEEE Photon. Technol. Lett.* 18(15), 1582-1584 (2006).
- [29] Bimberg, D., Posilovic, K., Kalosha, V., Kettler, T., Seidlitz, D., Shchukin, V. A., Ledentsov, N. N., Gordeev, N. Y., Karachinsky, L. Y., Novikov, I. I., Maximov, M. V., Shernyakov, Y. M., Chunareva, A. V., Bugge, F. and Weyers, M., "High-power high-brightness semiconductor lasers based on novel waveguide concepts," *Proc. SPIE 7616*, 76161I (2010).
- [30] Shchukin, V., Ledentsov, N., Posilovic, K., Kalosha, V., Kettler, T., Seidlitz, D., Winterfeldt, M., Bimberg, D., Gordeev, N. Y., Karachinsky, L. Y., Novikov, I. I., Shernyakov, Y. M., Chunareva, A. V., Maximov, M. V., Bugge, F. and Weyers, M., "Tilted Wave Lasers: A Way to High Brightness Sources of Light," *IEEE J. Quant. Electron.* 47(7), 1014-1027 (2011).
- [31] Bull, S., Larkins, E.C., Brand, T., Unger, A., Traub, M., Hengesbach, S., Uusimaa, P., Vilokkinen, V., Crump, P., Erbert, G., Lucas-Leclin, G., Georges, P., Rataj, T. and Deichsel, E., "The BRIDLE Project: High Brilliance Diode Lasers for Industrial Applications," *The Celebration of the 50th Anniversary of the Diode Laser*, University of Warwick, Coventry, UK, 20-21 September (2012).